



Published in final edited form as:

Nat Commun. ; 6: 7103. doi:10.1038/ncomms8103.

Inhibition of vemurafenib-resistant melanoma by interference with pre-mRNA splicing

Maayan Salton¹, Wojciech K. Kasprzak², Ty Voss¹, Bruce A. Shapiro³, Poulikos I. Poulikakos⁴, and Tom Misteli¹

¹National Cancer Institute, NIH, Bethesda MD, 20892

²Leidos Biomedical Research, Inc., Frederick National Laboratory, Frederick MD, 21702

³National Cancer Institute, NIH, Frederick MD, 21702

⁴Icahn School of Medicine at Mount Sinai, New York, NY, 10029

Abstract

Mutations in the serine/threonine kinase *BRAF* are found in more than 60% of melanomas. The most prevalent melanoma mutation is *BRAF*(V600E), which constitutively activates downstream MAPK signaling. Vemurafenib is a potent RAF kinase inhibitor with remarkable clinical activity in *BRAF*(V600E)-positive melanoma tumors. However, patients rapidly develop resistance to vemurafenib treatment. One resistance mechanism is the emergence of *BRAF* alternative splicing isoforms leading to elimination of the RAS-binding domain. Here we identify interference with pre-mRNA splicing as a mechanism to combat vemurafenib resistance. We find that small molecule pre-mRNA splicing modulators reduce *BRAF*³⁻⁹ production and limit *in-vitro* cell growth of vemurafenib-resistant cells. In xenograft models, interference with pre-mRNA splicing prevents tumor formation and slows growth of vemurafenib-resistant tumors. Our results identify an intronic mutation as a molecular basis for RNA splicing-mediated RAF inhibitor resistance and we identify pre-mRNA splicing interference as a potential therapeutic strategy for drug resistance in *BRAF* melanoma.

Introduction

The serine/threonine kinase *BRAF* is a proto-oncogene that acts in the MAP kinase pathway, connecting mitogen signals to transcriptional regulatory networks of cell proliferation. Mutations in *BRAF* are highly prevalent and are found in more than 60% of

Users may view, print, copy, and download text and data-mine the content in such documents, for the purposes of academic research, subject always to the full Conditions of use:http://www.nature.com/authors/editorial_policies/license.html#terms

Correspondence to: mistelit@mail.nih.gov.

The authors declare no competing financial interests, and no conflict of interest.

Supplementary information comprises figures 1–4 and table 1

Author contributions

MS and TM designed experiments, analyzed data and wrote the manuscript. MS performed and analyzed the data. TCV supported the experiment conducted using the high through-put imaging facility. WKK and BAS analyzed and plotted secondary structure. PIP helped design experiments.

melanomas (1–3). The most common melanoma mutation is BRAF(V600E) which constitutively activates downstream MAPK signaling (4).

Vemurafenib is a potent short-term therapeutic agent for treatment of BRAF(V600E)-positive melanoma⁵. However, patients invariably develop resistance to the drug^{6–15}. Resistance may arise by re-activation of MAP/ERK signaling pathways^{7, 11}, including upstream RAS activation by either RAS mutation, up-regulation of Receptor Tyrosine Kinases^{6, 14}, amplification of BRAF(V600E)¹², activating mutations in MEK⁸ and EGFR^{15, 16}. In ~30% of resistant tumors, resistance to the RAF inhibitor vemurafenib is conferred by alternative splicing via generation of BRAF isoforms lacking the RAS binding domain (RBD) encoded by exons 3–5^{17–19} (Fig. 1a). In the absence of the RBD, these BRAF isoforms dimerize even in the presence of low levels of RAS and confer drug resistance¹³.

Here we have explored the use of splicing modulation as a means to overcome vemurafenib resistance. We show that a point mutation in intron 8 of the BRAF gene mediates the resistance to vemurafenib in a drug-resistant cell line. Splicing modulation reverses aberrant BRAF splicing and slow growth of vemurafenib-resistant cells *in vitro* as well as *in vivo* using a xenograft model. Our results establish proof-of-principle for splicing modulation as a therapy for cancers with a molecular addiction to a weakly spliced oncogene isoform.

Results

Identification of an intronic BRAF mutation in vemurafenib-resistant C3 cells

To explore the molecular basis for the pre-mRNA splicing-mediated resistance to vemurafenib, we took advantage of the availability of vemurafenib-resistant C3 human melanoma cells¹³. These cells were generated by prolonged RAF inhibitor treatment of SKMEL-239 cells, a patient-derived melanoma cell line expressing BRAF(V600E)¹³. Similar to the situation in vemurafenib-resistant patients, resistance in C3 cells is mediated by expression of the alternatively spliced BRAF3-9 isoform, which lacks exons 4–8 (Fig. 1a)¹³. Consistent with the heterozygous nature of the BRAF(V600E) mutation, we detected both BRAF3-9 and fully spliced BRAF (BRAFF8-9) in the resistant C3 cells. No BRAF3-9 was detected in the parental cell line (Fig. 1b and Supplementary Fig. 1a). Elevated levels of BRAF3-9 in C3 cells were not due to nonsense-mediated degradation of other BRAF isoforms since silencing of UPF1, a component of the nonsense-mediated mRNA decay (NMD) complex, did not affect BRAF3-9 or 7–9 isoforms (Supplementary Fig. 1b, c; P value<0.01). Comparative sequencing of genomic BRAF in C3 and their parental SKMEL-239 cells identified a C-to-G mutation 51nt upstream of the 3' splice site (SS) of intron 8 in the BRAF(V600E) allele in C3 cells (Supplementary Fig. 1d). The –51 mutation maps to a predicted branch point (BP) in intron 8²⁰.

BRAF3-9 isoform formation by an intronic mutation

The –51 BRAF mutation was sufficient to promote BRAF3-9 formation. In a BRAF minigene containing exons 3, 4, 8, 9 and parts of introns 3 and 8 (Supplementary Fig. 1e),

the mutation favored production of the BRAF3-9 isoform ~ 2-fold and reciprocally reduced BRAF8-9 as judged by qPCR and semi-qPCR compared to the wild-type control (Fig. 1c, Supplementary Fig. 1g; P value<0.01). These effects were observed regardless of whether the reporters were introduced into parental or resistant C3 cells, excluding the possibility of cell-intrinsic effects on *BRAF* splicing (Supplementary Fig. 1h).

In addition to the predicted intron 8 BP, sequence analysis²⁰ and secondary structure analysis²¹ indicates the presence of two cryptic BPs (cBPs) located at positions –88 and –109 nt in intron 8, respectively, upstream of the 3' SS (Fig. 1d). To test whether these cBPs are responsible for BRAF3-9 splicing in the presence of the –51 mutation in vemurafenib-resistant cells, we mutated the cBPs in the context of either wt or mutant BRAF (Fig. 1e). Mutation of both putative cBPs in the wtBRAF background only had a negligible effect on BRAF3-9 splicing (Fig. 1e). In contrast, mutation of these sites in the context of the –51 vemurafenib-resistant BRAF mutant resulted in a 40% decrease in BRAF3-9 usage (Fig. 1e; P value<0.05). In addition mutation of a SRSF6 binding site at –129, but not of SRSF6 sites at exon 8, as well knockdown of SRSF6, but not SRSF1 or 3, in resistant C3 cells reduced endogenous BRAF3-9 by ~ 30% (Supplementary Fig. 1i and S1j; P value<0.05) and in U2OS cells stably expressing the BRAF minigene (Supplementary Fig. 1k and 1l; P value<0.01). No differences in SRSF6 mRNA levels were found in parental and resistant cell lines prior to RNAi treatment (Supplementary Fig. 1m).

Splicing modulators reduce BRAF3-9 production and activity

Given the shift in alternative splicing towards the BRAF3-9 isoform in vemurafenib-resistant cells, we tested whether treatment of resistant cells with the splicing modulator spliceostatin A (SSA)²² or its analog meayamycin B (MAMB)^{23, 24}, which target splicing factor SF3B1, inhibit BRAF3-9 formation. Treatment of C3-resistant cells with SSA (100ng; 9h) decreased the amount of BRAF3-9 in resistant C3 cells (Fig. 2a; P value<0.05). As a control, BRAF8-9 splicing was not affected by SSA treatment in either parental or resistant cell lines (Fig. 2a; Supplementary Fig. 2a). The effect of SSA was specific since ~60% reduction of its immediate target SF3B1 by RNAi (Supplementary Fig. 2b; P value<0.01) mimicked these effects (Supplementary Fig. 2c, d; P value<0.05). Treatment with MAMB (10nM; 9h) had similar effects (Fig. 2b; Supplementary Fig. 2e). As a further specificity control we monitored the AS of the MAPK gene *Erk-1*²⁵ and found no change in either parental or resistant cell lines (Supplementary Fig. 2f). As expected, reduction of BRAF3-9 splicing resulted in reduction of BRAF3-9 protein isoform in the resistant cell line (Fig. 2c) and was accompanied by a decrease in ERK signaling (Fig. 2d; Supplementary Fig. 2g, h; P value<0.05). As shown before¹³, total BRAF levels are lower in the resistant C3 cell line compared to parental (Fig. 2c), yet ERK activity is elevated in resistant cells (Fig. 2d; Supplementary Fig. 2g, h). We conclude that splicing interference antagonizes BRAF3-9 production.

Splicing modulators inhibit vemurafenib-resistant cell proliferation

As previously shown, vemurafenib-resistant C3 cells are dependent on BRAF3-9 for their proliferation¹³. To test whether splicing interference blocks proliferation of drug-resistant cells, we treated parental SKMEL-239 or resistant C3 cells for 3 days with MAMB. To

ensure cell survival over 3 days of treatment the dose range used (0.05–0.5nM) was ~50 times lower than the routine dose (10nM) used for short-term splicing assays²⁶. Resistant C3 cells were significantly more sensitive to MAMB compared to control parental cells in the absence of vemurafenib (Fig. 3a; P value<0.0001). The decreased proliferation rate in resistant C3 cells at a dose of 0.2 nM was accompanied by a reduction in the BRAF3-9 isoform (Supplementary Fig. 3a, b). Importantly, splicing interference re-sensitized resistant C3 cells to vemurafenib and reduced their proliferation potential to that of the drug-responsive parental cells (Fig. 3b; P value<0.001). Re-sensitization of C3 cells to vemurafenib was accompanied by a reduction of BRAF3-9 and consequently ERK signaling (Supplementary Fig. 3c, d; P value<0.05). Splicing modulation had no effect on proliferation, nor ERK signaling, in the parental cell line (Supplementary Fig. 3d, e). These results demonstrate that SSA and MAMB reduce BRAF3-9 splicing and consequently ERK signaling.

An estimated 30% of vemurafenib-resistant tumors contain various *BRAF* splicing isoforms^{13, 19} (Fig. 1a). To test whether splicing interference is specific to BRAF3-9 or is also applicable to other BRAF isoforms, we treated the vemurafenib-resistant M397AR cell line, which expresses BRAF1-11, with MAMB (10nM, 9h)^{12, 27}. BRAF1-11 was reduced by 50% in the resistant M397AR cells (Supplementary Fig. S3f; P value<0.05). This effect was not due to general splicing suppression since BRAF10-11 splicing was only moderately decreased by MAMB treatment in either M397 or M397AR cell lines (Supplementary Fig. 3f, g). As observed for C3 cells, resistant M397AR cells were more sensitive to MAMB compared to control M397 cells (Fig. 3c; P value<0.0001). Furthermore, splicing modulation had no effect on proliferation in two sets of cell lines resistant to vemurafenib by non-RNA splicing mediated mechanism^{14, 28} (Supplementary Fig. 3h, i).

Splicing modulation inhibits growth of vemurafenib-resistant tumors in vivo

To explore the potential use of splicing modulation in tumors *in-vivo*, we performed xenograft experiments. Parental SKMEL-239 or vemurafenib-resistant C3 cells (1×10^6) were injected subcutaneously into immunocompromised NSG mice and animals were treated with a low dose of SSA (0.28 μ g/kg; injected ip every 3 days). While SSA had no effect on tumor formation of parental cells, the formation of tumors by vemurafenib-resistant cells was effectively blocked in the presence of SSA (Fig. 4a; Supplementary Fig. 4a; P value<0.05). Vemurafenib-resistant tumors did not grow at all (3/4) or were at least 10 times smaller in weight than the average parental tumor (1/4). To probe whether splicing modulation has any beneficial effect on already established vemurafenib-sensitive or -resistant tumors NSG mice with clearly detectable 6 day old SKMEL-239 or C3 tumors were treated with vemurafenib alone or in combination with SSA (0.28 μ g/kg; ip injected every 3 days). As expected, vemurafenib reduced the size of SKMEL-293, but not of C3-tumors (Fig. 4b; Supplementary Fig. 4b;). SSA alone had no inhibitory effect and did not impede vemurafenib in drug-sensitive SKMEL-293 tumors (Fig. 4b). In contrast, SSA effectively inhibited tumor growth of vemurafenib-resistant C3 cells either alone or in combination with vemurafenib (Fig. 4b; Supplementary Fig. 4c; P value<0.05). Importantly, the reduction in tumor size observed in the resistant C3 tumors was accompanied by a decrease in BRAF3-9, but not BRAF8-9 (Fig. 4c; Supplementary Fig. 4d; P value<0.001).

We conclude that elimination of the resistance-causing BRAF3-9 isoform by interference with pre-mRNA splicing is an effective means to overcome vemurafenib-resistance *in-vivo*.

Discussion

We have here identified a point mutation in *BRAF* which renders melanoma cells vemurafenib-resistant. The mutation is located in a putative splicing branch-point and promotes the generation of the BRAF3-9 splicing isoform which confers vemurafenib resistance. We also find that several pre-mRNA splicing modulators, including SSA and MAMB, are able to counteract production of BRAF3-9 and overcome splicing-mediated vemurafenib resistance. The observed inhibitory effect of SSA on tumor formation of vemurafenib-resistant cells, even in the absence of the BRAF(V600E) inhibitor, indicates that elimination of the BRAF3-9 isoform is sufficient for a beneficial effect. This interpretation is in line with a dominant gain-of-function mechanism of BRAF3-9 which has constitutive BRAF activity due to loss of its RAS-binding domain¹³. Although the prevalence of the -51 mutation is currently unknown, targeting of RNA splicing-mediated resistance to vemurafenib will possibly be of general clinical relevance since ~30% of resistant tumors in patients treated with vemurafenib have been reported to express resistance-mediating BRAF splicing isoforms^{9, 13, 19}. Since all pre-mRNA splicing-mediated resistant tumors share common splicing isoforms that remove the RAS-binding domain in BRAF¹³, it is anticipated that splicing interference may be effective regardless of the precise resistance mutation. This notion is supported by our finding that splicing interference also prevents production of the vemurafenib-resistant BRAF1-11 isoform. The dose of splicing modulators used in our experiments is significantly lower than that used in previous clinical trials of the SSA/MAMB analogue E7107^{29, 30}, reducing the risk of toxicity and suggesting its feasibility in a clinical setting. In support, low doses of SSA had no effect on growth of parental cells or tumors and showed no discernible toxicity in mice. Our results suggest that inhibition of splicing may be a complementary approach to currently used combination therapies of vemurafenib with MEK or HDAC inhibitors^{14, 15, 31-33}. Given the high prevalence of pre-mRNA splicing-mediated drug resistance, targeting pre-mRNA splicing may be a useful approach to overcome drug resistance in melanoma patients.

Methods

Cell lines

SKMEL-239 parental and vemurafenib-resistant C3 cell lines (a kind gift from David Solit, MSKC) as well as M397/M397AR (a kind gift from Antoni Ribas, UCLA), WM938B/WM983B BR and 451 Lu/451 Lu BR cell lines (a kind gift from Meenhard Herlyn, The Wistar Institute) were grown in RPMI supplemented with 10% fetal bovine serum. U2OS (ATCC Number: HTB-96) cells were grown in DMEM supplemented with 10% fetal bovine serum; all cell lines were maintained at 37°C and 5% CO₂ atmosphere.

Sequencing

Sequencing was performed on purified PCR products of the 5' SS of intron 3 and 3' SS of intron 8 by GENEWIZ, Inc (MD).

BRAF reporter gene and transfection

The reporter gene was constructed by stitching PCR products using GeneArt Seamless Cloning Technology (Life Technologies), and the product cloned into the pEGFP-N1 vector (Clontech). PCR reactions used to create wtBRAF and mutBRAF reporters were constructed using genomic DNA of parental or resistant C3 cell lines as template, respectively. Mutagenesis was performed using QuikChange II XL Site-Directed Mutagenesis Kit (Agilent Technologies). Cells were transfected using Nucleofector Technology (Lonza). Primers used in this study are provided in Table 1.

RNAi

OnTarget Plus SMARTpool against SF3B1, UPF1, SRSF1, SRSF3 and SRSF6, were obtained from Dharmacon (Lafayette). Cells were grown to 20%–50% confluence and transfected with siRNA using the DharmaFECT 1 reagent (Lafayette).

qPCR

RNA was isolated from cells using the RNeasy plus mini kit (QIAGEN). cDNA synthesis was carried out with the High Capacity cDNA Reverse Transcription Kit (Applied Biosystems). qPCR was performed with the SsoFast EvaGreen Supermix (BioRad) on the Biorad iCycler. The comparative Ct method was employed to quantify transcripts, and delta Ct was routinely measured in triplicate. Primers used in this study are provided in Table 1. Erk1 and cErk1 primers were designed elsewhere²⁵.

Secondary structure, BP and SRSF6 binding site prediction

The full minigene sequence (2,684 nt) was folded using the Vienna RNAfold server (<http://rna.tbi.univie.ac.at/cgi-bin/RNAfold.cgi>)²¹ to obtain the minimum free energy (MFE) structure, the partition function and the base pairing probabilities. The results were cross-checked with the mfold server (<http://mfold.rna.albany.edu/?q=mfold>)^{34–36}. The 3' splice site of intron 8 (1000 nt) was analyzed using ESEfinder 3.0²⁰, to locate the BP as well as the two cBPs. The full minigene sequence (2,684 nt) was analyzed using ESEfinder 3.0²⁰ to identify possible binding sites for SRSF6.

Imaging

Cells were fixed by adding 4% paraformaldehyde in PBS directly into the culture medium at a 1:1 para:medium ratio and incubated for 15 min at RT. Cells were then washed 3× in PBS and stained with DRAQ5 (Biostatus Limited) 1:5,000 in PBS. Automated imaging steps were performed using an Opera system (Perkin Elmer). Images were taken using a 488/640 nm excitation laser (1st acquisition) and a 568 nm excitation laser (2nd acquisition). Images were analyzed using the Acapella software package (Perkin-Elmer). The Green/Red ratio was calculated as the ratio between the average nuclear intensity signal in the 488 nm

channel and the average nuclear signal in the 568 nm channel. Minimum of a 1000 nuclei were analyzed in each experiment condition.

Transplantation assays

Six-week-old male NOD/SCID/ interleukin 2 receptor γ null mice (NSG; The Jackson Laboratory) were maintained in pathogen-free conditions. For generation of tumors, cells (1×10^6 per injection) in 35 μ l of PBS were mixed with 15 μ l of Matrigel (BD BioScience) and were injected subcutaneously into the flanks of mice. Mice were locally shaved with a depilatory cream one day before injection. SSA (0.28 μ g/kg) was injected ip (100 μ l) every 3 days from the day indicated. Control mice were injected with PBS supplemented with methanol (SSA solvent). Vemurafenib analog PLX4720 mixed in chow (417 mg drug/kg chow; 67 mg/kg in mice) was provided from day 6 for the duration of the experiment. Tumor growth was assessed twice a week using a digital caliper. Tumor volume was calculated according to the formula d^2D , where d and D are the shortest and the longest diameter, respectively. At the endpoint, tumors were removed, weighted and RNA was extracted. All procedures were approved by the NIH Animal Use and Care Committee.

Proliferation assay

2000 cells were seeded per well in a 96 well plate; the cells were treated the next day. SSA, MAMB or vemurafenib (PLX4032, Selleck) were mixed to the indicated dose. Control cells were treated with both DMSO and methanol or DMSO alone, the solvents of PLX4032, SSA and MAMB, respectively. Proliferation was assessed after 3 days by CellTiter 96 (Promega) according to the manufacture instructions.

pERK1/2 assay

Meso Scale Discovery plate (MSD) was used for the detection of pERK1/2 and total ERK1/2, according to the manufacturer protocol. Plates were analyzed on the SECTOR Imager.

Immunoblotting

Immunoblotting was carried out according to standard techniques, briefly cells were harvested and lysed with RIPA lysis buffer supplemented with protease and phosphatase inhibitors, and the extracts were run on 4–12% Bis-Tris gel and transferred onto a polyvinylidene difluoride membrane. BRAF Antibody (F-7): sc-5284 (1:1000), Anti-Hsc70 antibody [1B5] (ab19136, 1:25,000).

Supplementary Material

Refer to Web version on PubMed Central for supplementary material.

Acknowledgments

We thank Paola Scaffidi and Travis Dittmer for advice and technical help, Antoni Ribas for the M397/M397AR cell lines, Meenhard Herlyn for 451Lu/451Lu BR and WM938B/WM983B BR cell lines, Minoru Yoshida for the kind gift of SSA, Plexxikon Inc for PLX4720, Kazunori Koide for MAMB, and Liang Cao for the use of the Sector Imager. This work was in part performed at the NCI High-Throughput Imaging Facility. This research was supported by the Intramural Research Program of the National Institutes of Health (NIH), NCI, Center for Cancer

Research and was funded in part with federal funds from the Frederick National Laboratory for Cancer Research, National Institutes of Health, under Contract HHSN261200800001E to WK.

References

1. Kudchadkar R, Paraiso KH, Smalley KS. Targeting mutant BRAF in melanoma: current status and future development of combination therapy strategies. *Cancer J*. 2012; 18:124–131. [PubMed: 22453012]
2. Pratilas CA, Solit DB. Targeting the mitogen-activated protein kinase pathway: physiological feedback and drug response. *Clinical cancer research : an official journal of the American Association for Cancer Research*. 2010; 16:3329–3334. [PubMed: 20472680]
3. Dhomen N, Marais R. BRAF signaling and targeted therapies in melanoma. *Hematology/oncology clinics of North America*. 2009; 23:529–545. ix. [PubMed: 19464601]
4. Wan PT, et al. Mechanism of activation of the RAF-ERK signaling pathway by oncogenic mutations of B-RAF. *Cell*. 2004; 116:855–867. [PubMed: 15035987]
5. Flaherty KT, et al. Inhibition of mutated, activated BRAF in metastatic melanoma. *The New England journal of medicine*. 2010; 363:809–819. [PubMed: 20818844]
6. Nazarian R, et al. Melanomas acquire resistance to B-RAF(V600E) inhibition by RTK or N-RAS upregulation. *Nature*. 2010; 468:973–977. [PubMed: 21107323]
7. Johannessen CM, et al. COT drives resistance to RAF inhibition through MAP kinase pathway reactivation. *Nature*. 2010; 468:968–972. [PubMed: 21107320]
8. Wagle N, et al. Dissecting therapeutic resistance to RAF inhibition in melanoma by tumor genomic profiling. *Journal of clinical oncology : official journal of the American Society of Clinical Oncology*. 2011; 29:3085–3096. [PubMed: 21383288]
9. Romano E, et al. Identification of Multiple Mechanisms of Resistance to Vemurafenib in a Patient with BRAFV600E-Mutated Cutaneous Melanoma Successfully Rechallenged after Progression. *Clinical cancer research : an official journal of the American Association for Cancer Research*. 2013
10. Sullivan RJ, Flaherty KT. Resistance to BRAF-targeted therapy in melanoma. *Eur J Cancer*. 2013; 49:1297–1304. [PubMed: 23290787]
11. Montagut C, et al. Elevated CRAF as a potential mechanism of acquired resistance to BRAF inhibition in melanoma. *Cancer research*. 2008; 68:4853–4861. [PubMed: 18559533]
12. Shi H, et al. Melanoma whole-exome sequencing identifies (V600E)B-RAF amplification-mediated acquired B-RAF inhibitor resistance. *Nature communications*. 2012; 3:724.
13. Poulidakos PI, et al. RAF inhibitor resistance is mediated by dimerization of aberrantly spliced BRAF(V600E). *Nature*. 2011; 480:387–390. [PubMed: 22113612]
14. Villanueva J, et al. Acquired resistance to BRAF inhibitors mediated by a RAF kinase switch in melanoma can be overcome by cotargeting MEK and IGF-1R/PI3K. *Cancer cell*. 2010; 18:683–695. [PubMed: 21156289]
15. Sun C, et al. Reversible and adaptive resistance to BRAF(V600E) inhibition in melanoma. *Nature*. 2014; 508:118–122. [PubMed: 24670642]
16. Girotti MR, et al. Inhibiting EGF receptor or SRC family kinase signaling overcomes BRAF inhibitor resistance in melanoma. *Cancer discovery*. 2013; 3:158–167. [PubMed: 23242808]
17. Wellbrock C, Karasarides M, Marais R. The RAF proteins take centre stage. *Nature reviews Molecular cell biology*. 2004; 5:875–885. [PubMed: 15520807]
18. Freeman AK, Ritt DA, Morrison DK. The importance of Raf dimerization in cell signaling. *Small GTPases*. 2013; 4
19. Shi H, et al. Acquired resistance and clonal evolution in melanoma during BRAF inhibitor therapy. *Cancer discovery*. 2014; 4:80–93. [PubMed: 24265155]
20. Cartegni L, Wang J, Zhu Z, Zhang MQ, Krainer AR. ESEfinder: A web resource to identify exonic splicing enhancers. *Nucleic acids research*. 2003; 31:3568–3571. [PubMed: 12824367]
21. Gruber AR, Lorenz R, Bernhart SH, Neubock R, Hofacker IL. The Vienna RNA websuite. *Nucleic acids research*. 2008; 36:W70–74. [PubMed: 18424795]

22. Nakajima H, et al. New antitumor substances, FR901463, FR901464 and FR901465. II. Activities against experimental tumors in mice and mechanism of action. *The Journal of antibiotics*. 1996; 49:1204–1211. [PubMed: 9031665]
23. Bonnal S, Vigevani L, Valcarcel J. The spliceosome as a target of novel antitumour drugs. *Nature reviews Drug discovery*. 2012; 11:847–859. [PubMed: 23123942]
24. Albert BJ, Sivaramakrishnan A, Naka T, Czaicki NL, Koide K. Total syntheses, fragmentation studies, and antitumor/antiproliferative activities of FR901464 and its low picomolar analogue. *Journal of the American Chemical Society*. 2007; 129:2648–2659. [PubMed: 17279752]
25. Aebersold DM, et al. Extracellular signal-regulated kinase 1c (ERK1c), a novel 42-kilodalton ERK, demonstrates unique modes of regulation, localization, and function. *Molecular and cellular biology*. 2004; 24:10000–10015. [PubMed: 15509801]
26. Albert BJ, et al. Meayamycin inhibits pre-messenger RNA splicing and exhibits picomolar activity against multidrug-resistant cells. *Molecular cancer therapeutics*. 2009; 8:2308–2318. [PubMed: 19671752]
27. Lassen A, et al. Effects of AKT inhibitor therapy in response and resistance to BRAF inhibition in melanoma. *Molecular cancer*. 2014; 13:83. [PubMed: 24735930]
28. O’Connell MP, et al. Hypoxia induces phenotypic plasticity and therapy resistance in melanoma via the tyrosine kinase receptors ROR1 and ROR2. *Cancer discovery*. 2013; 3:1378–1393. [PubMed: 24104062]
29. Kotake Y, et al. Splicing factor SF3b as a target of the antitumor natural product pladienolide. *Nature chemical biology*. 2007; 3:570–575. [PubMed: 17643112]
30. Eskens FA, et al. Phase I, Pharmacokinetic and Pharmacodynamic Study of the First-in-Class Spliceosome Inhibitor E7107 in Patients with Advanced Solid Tumors. *Clinical cancer research : an official journal of the American Association for Cancer Research*. 2013
31. Park SJ, et al. The MEK1/2 Inhibitor AS703026 Circumvents Resistance to the BRAF Inhibitor PLX4032 in Human Malignant Melanoma Cells. *The American journal of the medical sciences*. 2013
32. Flaherty KT, et al. Combined BRAF and MEK inhibition in melanoma with BRAF V600 mutations. *The New England journal of medicine*. 2012; 367:1694–1703. [PubMed: 23020132]
33. Johannessen CM, et al. A melanocyte lineage program confers resistance to MAP kinase pathway inhibition. *Nature*. 2013
34. Zuker M. Mfold web server for nucleic acid folding and hybridization prediction. *Nucleic acids research*. 2003; 31:3406–3415. [PubMed: 12824337]
35. Waugh A, et al. RNAML: a standard syntax for exchanging RNA information. *RNA*. 2002; 8:707–717. [PubMed: 12088144]
36. Mathews DH, Sabina J, Zuker M, Turner DH. Expanded sequence dependence of thermodynamic parameters improves prediction of RNA secondary structure. *Journal of molecular biology*. 1999; 288:911–940. [PubMed: 10329189]

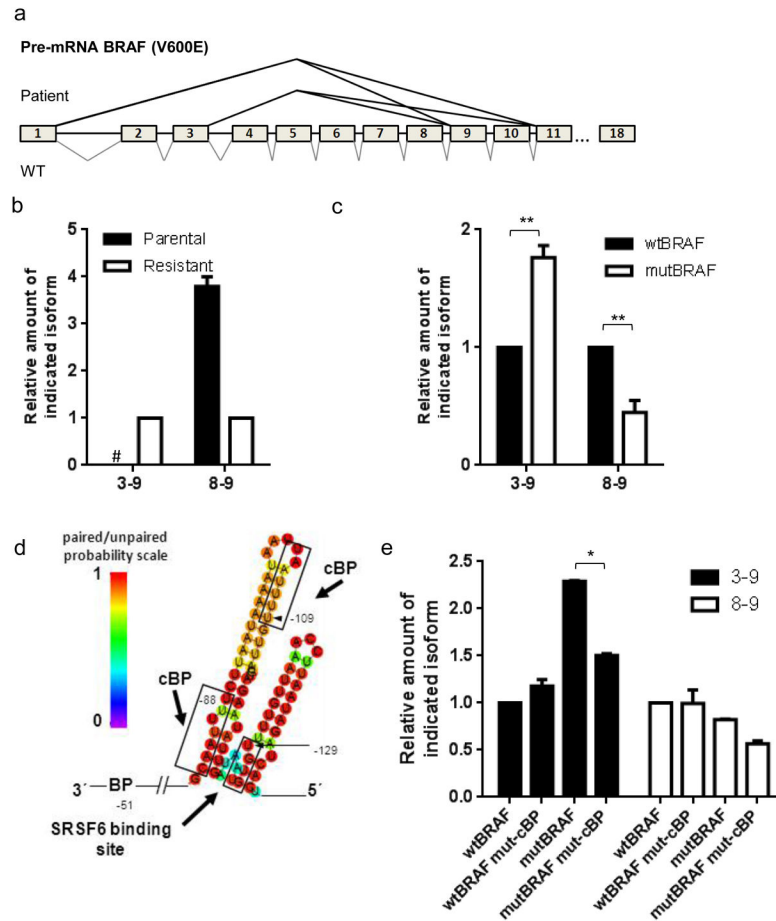


Figure 1. A branch-point mutation in the resistant C3 cell line promotes BRAF3-9 splicing
a. Schematic representation of AS events detected in vemurafenib-resistant melanoma patients. Only introns are drawn to scale, intron 1 = 63 kbp. **b.** Quantitative qPCR analysis of parental and resistant C3 cells. Indicated values represent isoform values normalized to total BRAF mRNA. Isoform levels in resistance C3 cell line was set to 1, #: signal below detection limit. **c.** U2OS cells were transfected with wt or mutant BRAF reporter. mRNA levels were assessed after 48hr using qPCR, indicated values represent isoform values normalized to the total amount of GFP mRNA. Isoform levels in wtBRAf were set to 1. **d.** Secondary structure of the 3' SS of intron 8. Color-coded pairing probability of individual nucleotides is indicated. **e.** U2OS cells were transfected with the indicated BRAF reporter. mRNA levels were assessed after 48hr using qPCR, BRAF3-9 isoform values are normalized to the total amount of GFP mRNA. Isoform levels in wtBRAf were set to 1. (**b**, **c** and **e**) Values represent the means of three independent experiments \pm SD (* P <0.05, ** P <0.01, t-test).

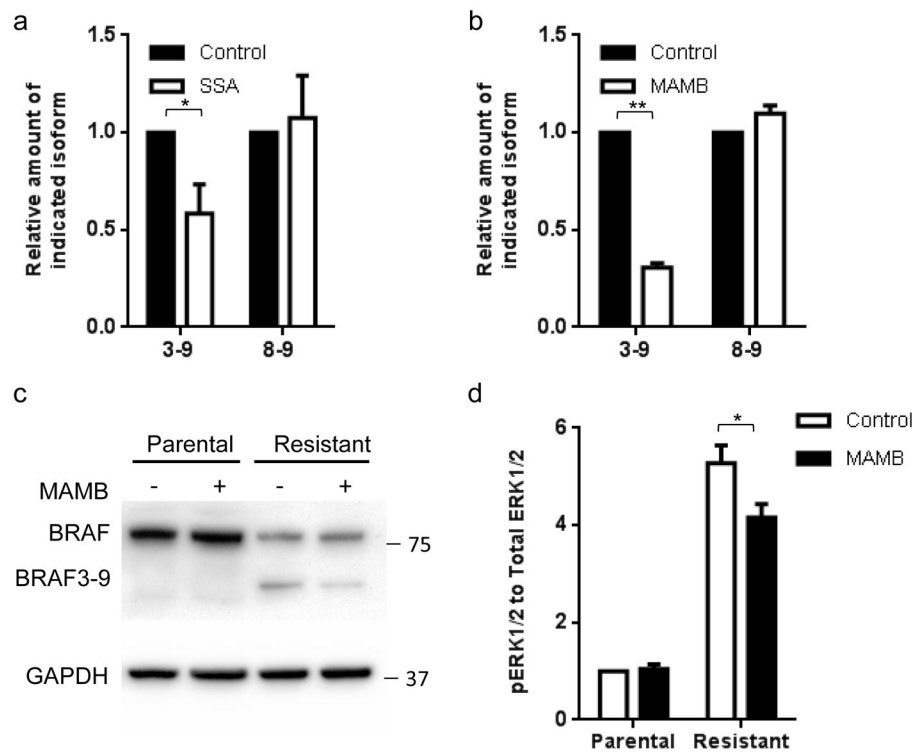


Figure 2. Effect of splicing modulation on BRAF3-9 splicing

a. Vemurafenib-resistant C3 cells were treated with 100ng/ml SSA for 9 hours. mRNA levels were assessed using qPCR. Indicated isoform values are normalized to total BRAF mRNA. Isoform levels in the control were set to 1. **b.** Vemurafenib-resistant C3 cells were treated with 10nM MAMB for 9 hours. mRNA levels were assessed using qPCR. Indicated isoform values are normalized to total BRAF mRNA. Isoform levels in the control were set to 1. **c and d.** Parental and resistant C3 cells were treated with 10 nM MAMB for 9 hours. **(c)** Immunoblotting was conducted with the indicated antibodies, **(d)** BRAF activity was determined by measuring pERK1/2 levels using a Meso Scale Discovery (MSD) technology. For SSA, MAMB experiments control cells were treated with either methanol or DMSO, the compound solvent. **(a, b and d)** Values represent means of three independent experiments \pm SD (*P<0.05, **P<0.01, t-test).

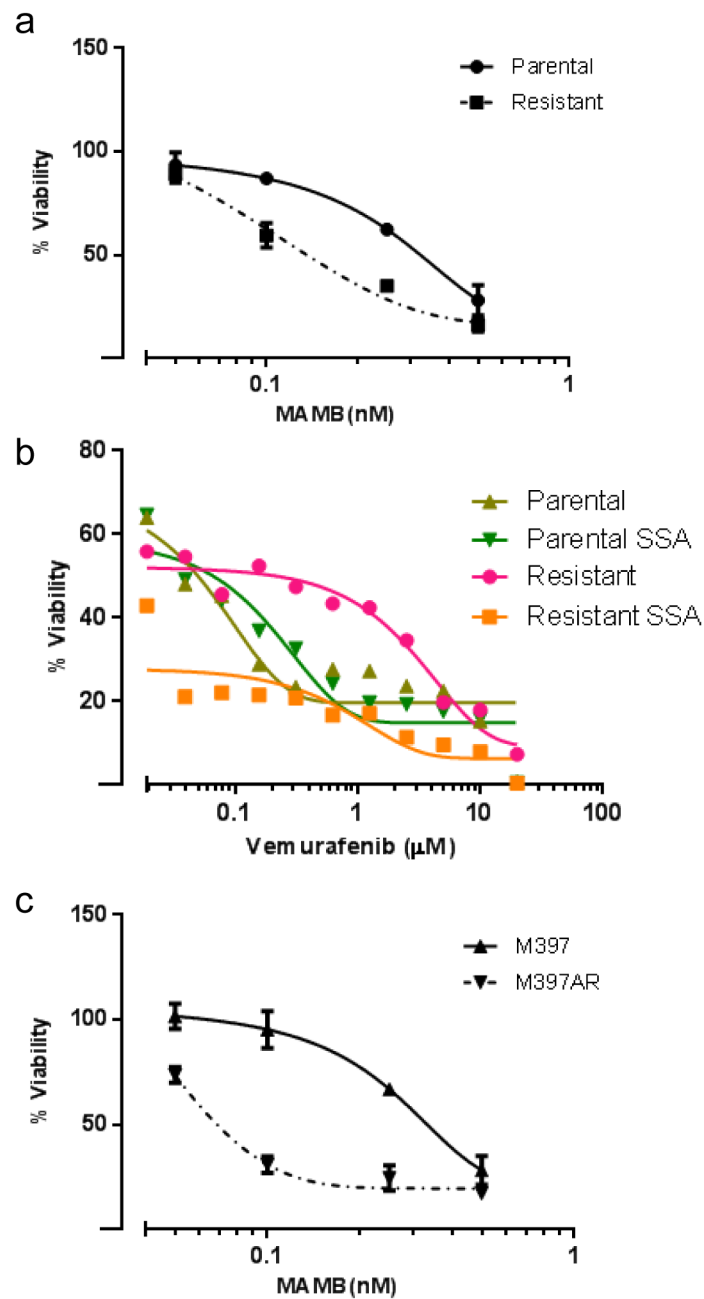


Figure 3. Splicing modulation perturbs proliferation of resistant cell lines

a. Parental and resistant C3 cells were treated with the indicated concentration of MAMB and cell viability was determined after 3 days. **b.** Vemurafenib sensitivity curves at 3 days for parental and resistant C3 cells in the presence or absence of 1 ng/ml of SSA. **c.** Parental M397 and resistant M397AR cells were treated with the indicated concentration of MAMB and cell viability was determined after 3 days. Values represent means of 3 independent experiments \pm SD ($P < 0.001$, two-way ANOVA).

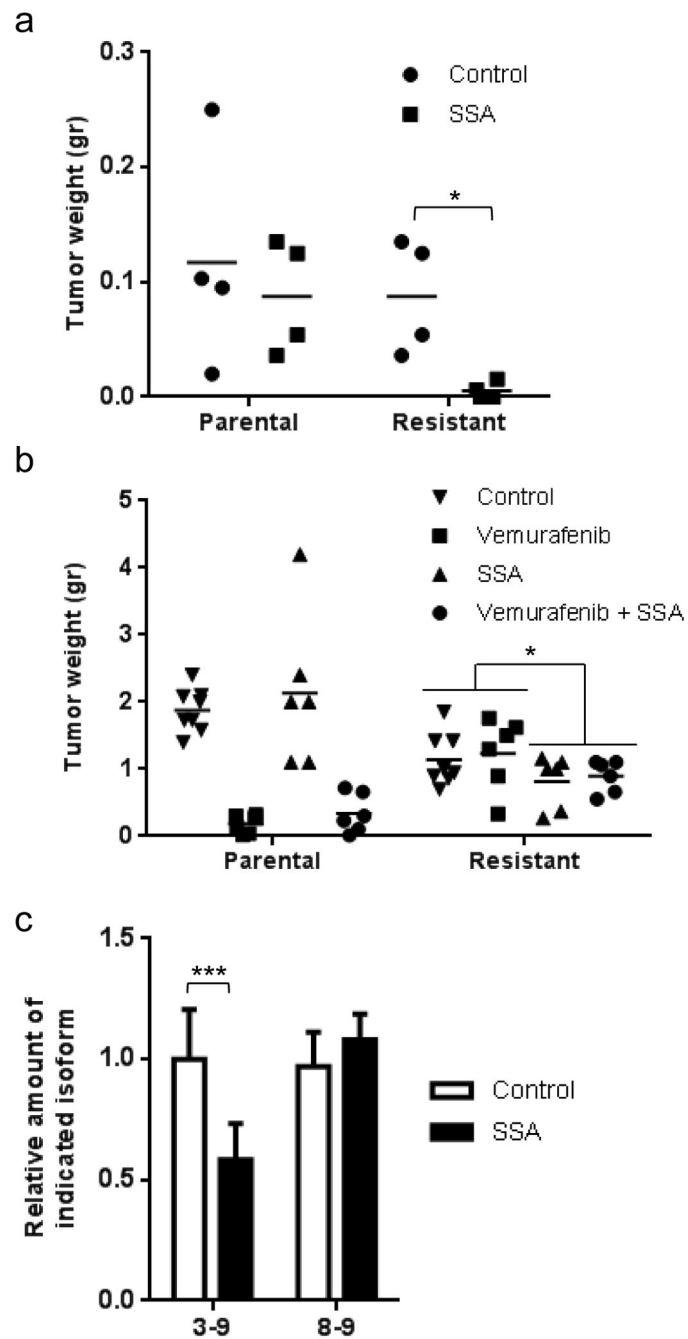


Figure 4. SSA inhibits tumor growth of vemurafenib-resistant cells

a. Values of tumor weight at the experiment endpoint (day 20) represent means \pm SEM from 4 mice (* P <0.05, t-test). **b.** Tumors were formed for 6 days by injection of parental or resistant C3 cells and NSG mice then treated with vemurafenib analog PLX4720 mixed in chow (417 mg drug/kg chow; 67 mg/kg in mice) and/or 0.28 μ g/kg SSA. Values of tumor weight at the experiment endpoint (day 35) represent means \pm SEM from 6 mice (* P <0.05, t-test). **c.** Quantitative PCR analysis of resistant C3 tumors with or without SSA. mRNA

values are normalized to total BRAF mRNA. Control was set to 1. Values represent means of 6 mice \pm SD (**P<0.001, t-test).

Author Manuscript

Author Manuscript

Author Manuscript

Author Manuscript